

# Investigating the Mechanical Properties of Al 7075 Alloy for Automotive Applications: Synthesis and Analysis

J, Kumaraswamy

Dept. of Mechanical Engineering, R. L. Jalappa Institute of Technology

Anil K C

Dept. of Industrial Engineering and Management, Siddaganga Institute of Technology

T R Veena

Dept. of Industrial Engineering and Management, Siddaganga Institute of Technology

Purushotham, G.

Dept. Aeronautical Engineering, Gopalan College of Engineering and Management

他

<https://doi.org/10.5109/7151674>

---

出版情報 : Evergreen. 10 (3), pp.1286-1295, 2023-09. 九州大学グリーンテクノロジー研究教育センター

バージョン :

権利関係 : Creative Commons Attribution-NonCommercial 4.0 International

# Investigating the Mechanical Properties of Al 7075 Alloy for Automotive Applications: Synthesis and Analysis

Kumaraswamy J<sup>1\*</sup>, Anil K C<sup>2</sup>, T R Veena<sup>3</sup>, G. Purushotham<sup>4</sup>, Sunil Kumar K<sup>5</sup>

<sup>1</sup>Dept. of Mechanical Engineering, R. L. Jalappa Institute of Technology, Doddaballapur, Karnataka, India.

<sup>2, 3</sup>Dept. of Industrial Engineering and Management, Siddaganga Institute of Technology, Karnataka, India.

<sup>4</sup>Dept. Aeronautical Engineering, Gopalan College of Engineering and Management, Bangalore

<sup>5</sup>Dept. of Mechanical Engineering, R. L. Jalappa Institute of Technology, Doddaballapur, Karnataka, India.

E-mail: kumaraswamyj@rljit.in

(Received June 20, 2023; Revised August 4, 2023; accepted August 22, 2023).

**Abstract:** Due to their low weight, high strength and enhanced tribological properties, aluminium alloy composite materials are recognized globally after for highly scientific applications. Al7075 hybrid composite was created by using the sand mould process in an electric resistance furnace to reinforce aluminium oxide (Al<sub>2</sub>O<sub>3</sub>) and boron carbide (B<sub>4</sub>C) particles. In this study, the mechanical behaviour of hybrid composites made of Al7075, Al<sub>2</sub>O<sub>3</sub>, and B<sub>4</sub>C with stable Al<sub>2</sub>O<sub>3</sub> contents of 2% and variable B<sub>4</sub>C weight percentages of 2% to 6% was examined. In both pure and cast specimens, the mechanical characteristics, such as tensile and compressive strength, hardness, and microstructure analysis, were assessed. In this study, the mechanical characteristics of the hybrid composites made from Al7075 alloy were experimentally studied and validated using the ASTM standard and FEA. The results showed that when hard ceramic particles (Al<sub>2</sub>O<sub>3</sub>/B<sub>4</sub>C) were added to a matrix alloy (Al7075), mechanical characteristics such as compressive strength and hardness improved while tensile strength was reduced. The static structural tensile test was successfully simulated in ANSYS. It was observed that both FEA results and analytical results were correlated.

Keywords: Al7075; Al<sub>2</sub>O<sub>3</sub>/B<sub>4</sub>C; Microstructure; Mechanical behaviour; FEA

## 1. Introduction

Materials for cutting-edge technology need to combine a number of features that aren't present in regular metal alloys and reinforcing materials. Using composite materials is becoming more popular in order to get better performance. In response to the need for materials with more strength and capacities at cheaper costs, advanced composite materials have arisen. Composite materials may be able to overcome the limitations of conventional alloys and monolithic materials. By incorporating reinforcements like ceramics, oxides, and carbides into the base material, it is possible to create distinctive materials with improved performance. The ideal material combination is determined by the specific application and the proportionate weight given too many factors, including stiffness, strength to weight ratio, fatigue, wear resistance, and thermal expansion<sup>1-2</sup>). It has been discovered via research into the mechanical and tribological properties of various reinforcements that they enhance tensile strength, hardness, wear resistance, and corrosion resistance in a range of applications. TiC, B<sub>4</sub>C, Al<sub>2</sub>O<sub>3</sub>, SiC, and Si<sub>3</sub>N<sub>4</sub> are only a few of the materials utilised in fortification, which is often done with metal or

ceramic particles<sup>3-5</sup>). Many techniques, such as fluid synthesis, solid-state manufacture, metal injection moulds, grinding mixing, and mechanical assemblages, can be used to produce metallic lattice blends. Nickel composites are frequently utilised in space, marine, and turbine motors because of their mechanical properties and related attributes at high temperatures. However, its employment in further applications is restricted because of its high density and poor creep resistance<sup>6-8</sup>). Composites offer a workable solution to issues with nickel amalgams by reducing thickness and enhancing the mechanical properties of the nickel lattice at high temperatures. They are therefore the preferred material for the syphon, valve, maritime, and aviation industries. Yet, their development is essential for the expansion and development of hybrid metal matrix composites for the manufacture of vehicles<sup>9-12</sup>). High-purity aluminium oxide (Al<sub>2</sub>O<sub>3</sub>) is a potentially appealing embedding medium for base metallic materials because to its remarkable wear resistance, high biocompatibility, minimal friction, moderate wear resistance, and high purity. It is acknowledged that alumina-TiN composites are suitable for use in the aerospace and automotive industries. It is anticipated that TiN, when evenly and finely diffused within the alumina

lattice, will reinforce the composite while also enhancing its flexural quality and fracture toughness, boosting its intrinsic qualities. As the sand grain fineness number increases, the tensile strength of A713 Alloy casting decreases, and the presence of voids between the grains increases total permeability. In the as-cast condition, the tensile strength of the Al-Cu-Mg alloy increases with magnesium content, according to<sup>13-15</sup>. The ratios of fly ash and e-glass fibre also boosted the tensile strength of the Al7075 alloy. Regrettably, when the reinforcement (fly ash and e-glass) was added to the Al7075 alloy in amounts more than 3%, it proved challenging to mix and stir the molten metal to achieve uniformity. When compared to the material as-cast, the tensile strength of the Al7075 alloy for reinforced particles and heat-treated composites rose by 32%. Al7075/SiC composite showed a higher UTS than Al7075 matrix for rheoformed cylinder components, according to<sup>16-27</sup>.

The evaluated the mechanical characteristics of composites made from Al 6xxx + magnesium and rock dust using the Stir casting technique while altering the weight percentages<sup>28</sup>. The findings showed that the inclusion of rock dust decreased composite density while the addition of AZ31 increased tensile strength. A review of the effect of ceramic particles on the microstructural and mechanical properties of aluminium composites<sup>29</sup>. The results showed that the tensile and hardness strength of the MMCs improved as the reinforcing content increased<sup>30</sup>. Furthermore, found that the wear rate rose with greater loads but decreased with the addition of carbide particles. The studied the effect of cenospheric particles on the micro-structure and mechanical behaviour of Al composites<sup>31</sup>.

## 2. Materials & Fabrication

### 2.1 Aluminium 7075 alloy.

The chosen reinforcement materials for MMCs were alumina (Al<sub>2</sub>O<sub>3</sub>) and boron carbide (B<sub>4</sub>C), along with the Al 7075 alloy as the matrix. Table 1 lists the chemical composition of Al7075.

Table 1. Element configuration of Al7075 alloy

Element	Composition %
Mg	2.5
Fe	0.5
Cr	0.23
Mn	0.3
Al	88.6
Cu	1.6
Ti	0.2
Zn	5.6
Si	0.4
Cr	0.23

Alumina, also called aluminum oxide (Al<sub>2</sub>O<sub>3</sub>), is a remarkably pure ceramic material widely utilized in

diverse applications owing to its adaptable properties. One of its most frequent uses is in polishing as an abrasive, and it has diverse particulate sizes that allow flexibility for fluoro coating formulators. A tailored matrix can be used to change the wide variety of alumina materials' unique property profiles. Electrical insulation, high compressive strength, outstanding thermal conductivity, great wear and corrosion resistance, and low density are only a few of its characteristics. Alumina is a white powder that resembles table salt, is chemically stable, and has a melting point above 2050°C. Moreover, it is the hardest refractory material utilised in manufacturing and is widely used in dense fused cast alumina blocks as a glass interaction refractory [2, 4].

Boron carbide (B<sub>4</sub>C) is a highly versatile ceramic material that possesses exceptional thermal stability and a high melting point, making it ideal for use in refractory applications. Its abrasion resistance also renders it suitable for use in coatings and abrasive powders. Additionally, boron carbide's low density and high hardness make it a top performer in ballistic applications, commonly utilized in nuclear applications. It is renowned as a robust material that provides excellent shielding against neutrons and stability to ionizing radiation due to its high hardness. With its attractive properties, including low density, high strength, and good chemical stability, boron carbide is widely recognized as one of the most exceptional ceramic materials available.

### 2.3 Casting and Testing.

Alumina and B<sub>4</sub>C were used as reinforcements to prepare the composites. The Al<sub>2</sub>O<sub>3</sub> content was kept constant at 2%, whereas the B<sub>4</sub>C content was varied from 2% to 6% in increments of 2% by weight. After adding Al<sub>2</sub>O<sub>3</sub> and B<sub>4</sub>C particles through a vortex generated by an alumina-coated stainless-steel stirrer, the molten metal pool was stirred at 200-300 rpm for 15 minutes using a zirconium-coated stirrer. The resultant slurry was then used to create the composite materials by pouring it into heated permanent moulds.

The polished composite samples prepared using a Kroll reagent in accordance with E3 11 ASTM were scanned using an NIKON-ECLIPSE LV 150 Japan optical metallurgical microscope to investigate the uniform dispersion of particles in the composite. Tensile testing was conducted using a UTM with a 400 kN maximum load capacity, and the tensile specimens were created following the ASTM E8 standard. The highest tensile strength was measured using an electronic tensometer (Model: TUE-C-400). To conduct a hardness test, a Brinell hardness machine was used according to the ASTM E8M-16a specifications on the prepared hardness specimens, which had dimensions of diameter 20 mm and length 15 mm. The wear samples, with a diameter of 10 mm and length of 30 mm, were prepared in accordance with G99 ASTM (Model: WTE 165 and Version-EV00).

### 3. Results and Discussion

The current research on microstructure includes conducting tensile, compression, and hardness tests in accordance with ASTM standards.

#### 3.1 Microstructure study.

Figures 1(a) and 1(b) depict microscopic pictures of Al alloy and Al-based hybrid matrix composites (b). Understanding the mechanical properties and potential uses of aluminium hybrid composites reinforced with boron carbide and aluminium oxide particles depends critically on the microstructure characterization. The molten aluminium pool was stirred into a vortex by an alumina-coated stainless steel stirrer in order to introduce  $\text{Al}_2\text{O}_3$  and  $\text{B}_4\text{C}$  particles. Before being put into heated permanent moulds, the molten metal was first stirred for 15 minutes at 200-300 rpm with a zirconium-coated stirrer. Many methods, including scanning electron microscopy (SEM), energy-dispersive X-ray spectroscopy (EDS), and X-ray diffraction, were used to analyse the microstructure of the composites (XRD). The composites homogeneous distribution of reinforcing particles throughout the aluminium matrix was visible in SEM pictures. The EDS examination verified that  $\text{Al}_2\text{O}_3$  and  $\text{B}_4\text{C}$  particles were present in the composites. The results of the X-ray diffractometry (XRD) examination further supported the existence of the reinforcing particles and showed that the composites had stable  $\text{Al}_2\text{O}_3$  contents of 2% and  $\text{B}_4\text{C}$  contents varying from 2% to 6% in steps of 2% by weight.

The microstructure analysis also revealed that the  $\text{B}_4\text{C}$  particle addition caused the aluminium matrix's grain size to become finer.

The nucleation of new grains around the  $\text{B}_4\text{C}$  particles is blamed for the reduction in grain size. The inclusion of  $\text{B}_4\text{C}$  particles significantly enhanced the interfacial connection between the reinforcing particles and the aluminium matrix, according to the microstructure study. The development of a reaction layer between the reinforcing particles and the aluminium matrix is blamed for the increased interfacial bonding.

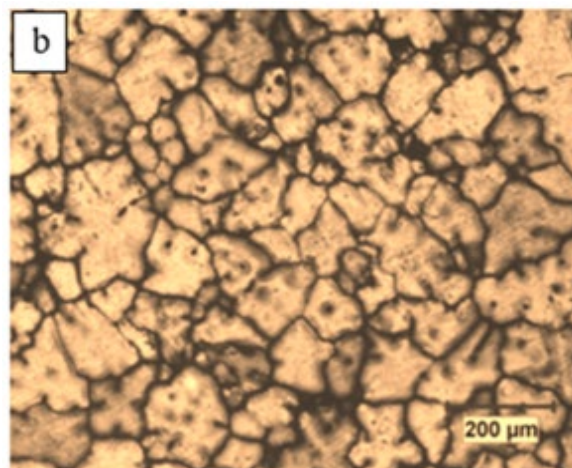
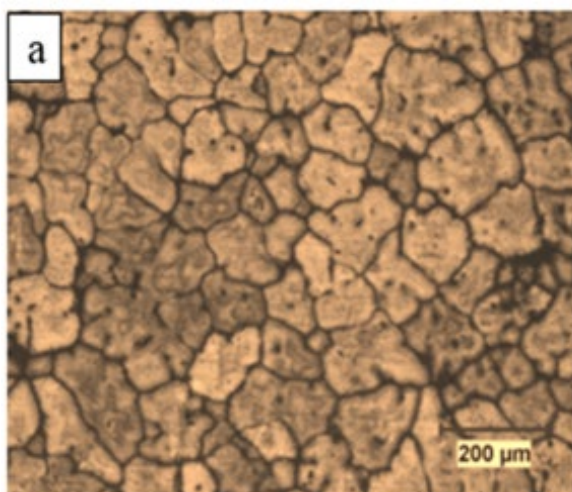


**Fig. 1:** Microstructure analysis; a) Al 7075 alloy, b) Al+ 2%  $\text{Al}_2\text{O}_3$ + 4%  $\text{B}_4\text{C}$  hybrid composites.

The microstructure analysis of the hybrid aluminium composites reinforced with boron carbide and aluminium oxide particulates showed that they had a uniform distribution of the reinforcing particles within the aluminium matrix, a stable  $\text{Al}_2\text{O}_3$  content of 2%, and  $\text{B}_4\text{C}$  content ranging from 2% to 6% in increments of 2% by weight. The addition of  $\text{B}_4\text{C}$  particles increased the interfacial connection between the reinforcing particles and the aluminium matrix and refined the grain size of the aluminium matrix. The design and development of innovative lightweight materials with improved mechanical properties will be significantly impacted by these findings.

#### 4.2 Tensile strength

The tensile strength of both unreinforced Al alloy samples and hybrid composite samples were examined and the outcomes are demonstrated in Figure 2. The figure displays that the composites have the capability to sustain considerably higher loads in comparison to the alloys, which can be credited to the addition of reinforced particles that result in a substantial increase in tensile strength.

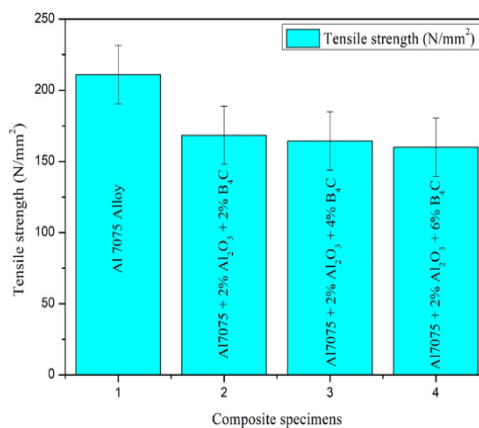


**Fig. 2:** Tensile strength of the hybrid composite

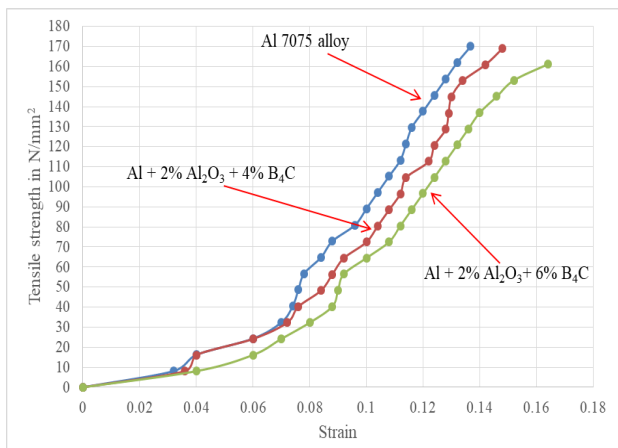


Fig. 3: Stress-Strain curve of the composites.

4.3 Compression Strength

The developed hybrid composites underwent compression tests in accordance with ASTM-E8 standards. The results indicated that an increase in the weight percent of reinforcement enhanced compressive strength. As seen in Figure 4, the composites' compressive strength significantly increased as compared to the base alloy after the addition of alumina and boron particles. The interfacial connection between the matrix and the reinforcements was said to be responsible for this enhancement [7]. The base matrix's stiffer reinforcement particles functioned as obstacles, preventing the alloy's plastic flow and dislocation motion.

As seen in Figure 3, the presence of solid B<sub>4</sub>C/Al<sub>2</sub>O<sub>3</sub> reinforcing components with superior mechanical properties caused the hybrid composites' tensile strength to decline significantly when compared to the unreinforced Al alloy. These supporting components provide the dual purposes of resisting and transferring the applied tensile force. By strengthening their bonds with the nearby metal matrix atoms, they increase the base alloy's strength by preventing dislocation and reinforcing the unreinforced material

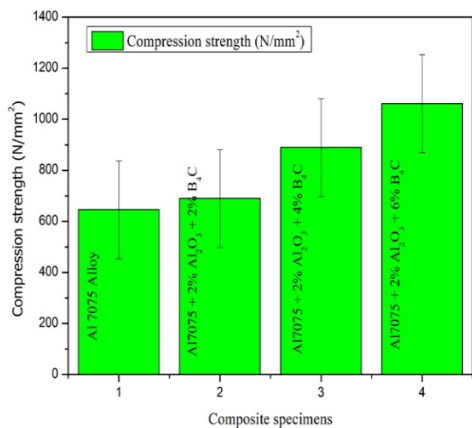


Fig. 4: Compression strength

The hybrid MMCs' compressive strength was higher than that of the monolithic due to the uniform dispersion

of reinforcing particles in the Al alloy. According to Figure 5, and in line with the findings of other researchers [4], the compressive strength of the hybrid MMCs dropped as the B<sub>4</sub>C level rose. Researchers [6] have confirmed that B<sub>4</sub>C works well as a solid lubricant for enhancing compression stability, but they have also found that robustness is negatively impacted. The observed decrease in compressive strength can be the result of B<sub>4</sub>C-induced mechanisms like particle pull-out and crack propagation [8].

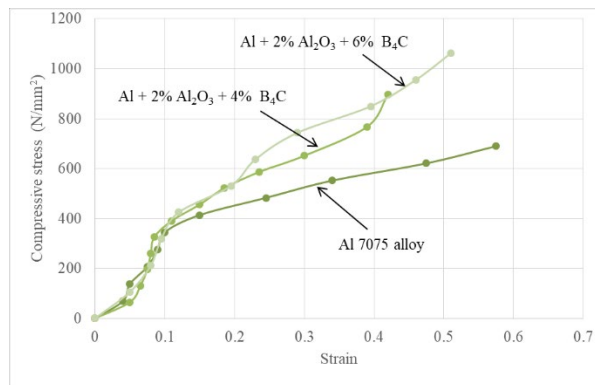


Fig. 5: Stress-Strain curve of the compressive strength composites.

4.4 Hardness

After performing a hardness test on the prepared samples, it was observed that the hybrid composite (223.92 BHN) exhibited greater hardness compared to the base metal alloys (170 BHN). Particle strengthening, grain boundary strengthening, and dispersion strengthening are only a few of the strengthening techniques that are responsible for the increase in hardness. By using these techniques, the amount of reinforcing particles in the metal matrix solution was increased. The hard ceramic boron carbide particles were incorporated in order to serve as reinforcements in the supple, stretched metal matrix. This stopped atoms from dislocating and made materials more resistant to plastic deformation.

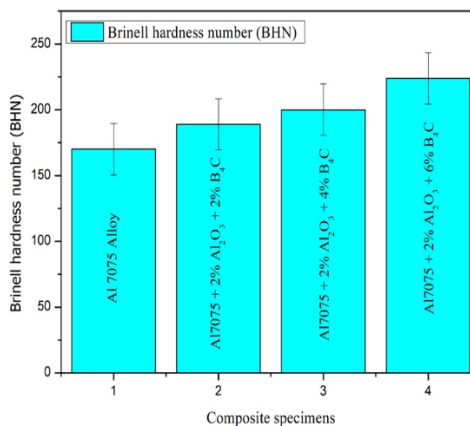


Fig. 6: Hardness of the composites.

The results demonstrate that the introduction of these

strong reinforcing particles greatly improved the composite's overall hardness. According to the observation, the reinforcement of the framework with fortifications led to an increase in weight proportion. This resulted in a decrease in the power of molecule separation, leading to an intensification of grain limit obstruction and increased solidity. According to Figure 6, the composites are harder than both standard aluminium alloys and aluminium alloys with 2%  $\text{Al}_2\text{O}_3$  and 6%  $\text{B}_4\text{C}$ , which suggests that they are more rigid than other hybrid composites with different weight ratios.

#### 4.4 Fractured surfaces Analysis

The evaluation of morphological features such dimples, transgranular sides, void nucleation, and crack formation were made possible by the investigation of the disruption surfaces using elastic samples. The unreinforced Al alloy and hybrid composite (as shown in Figure 7) formed separately in an uncontrolled mixture and a hybrid blend, respectively, on the fracture surface, according to the examination of FE-SEM images.

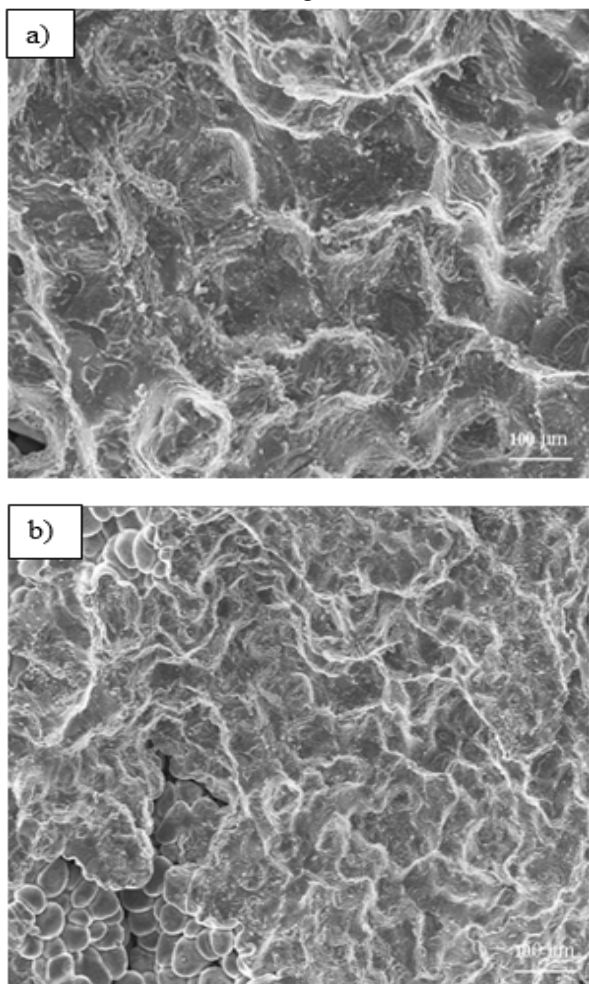


**Fig. 7:** FE-SEM of fractured surfaces of a) Al 7075 alloy, b) Al+ 2%  $\text{Al}_2\text{O}_3$  + 6%  $\text{B}_4\text{C}$  hybrid composites.

It was clear from a comparison of the two fracture surfaces that the hybrid material had much less voids than

the unreinforced composite. Also, the position of the fracture was significantly influenced by the quantity of voids that were present in the composite system. Notably, the voids within the composite system were considerable, and they remained unfilled. The number of holes present in the composite structure was lower compared to the amalgams. This was due to the use of stiffeners, which filled up the holes in the composite. As a result, the composite became less flexible when on the ground. However, both the composite and split structures exhibited small breaks due to the formation of micro voids. The composite structure was better equipped to handle the formation of these breaks due to the presence of an adaptable metal network that provided fortifications. The increased bonding strength between the fortifying particles and the network at the network/strengthening interface caused the break in the composite, rather than at the interface itself. Despite the improved pressure convection, the stiffeners were not able to transfer the convection effectively. As a result, the hardening materials experienced weak splits regularly, and the Al combination grid was subjected to malleable pounding.

#### 4. Optimization of the mechanical properties

Finite Elements Analysis (FEA) was carried out to mitigate the tensile test and compression test simulated on ANSYS workbench software. A 3D Model specimen was prepared as per the ASTM standard dimensions in a CAD software and then imported to the ANSYS software.

##### 4.1 Tensile

The geometric entity was converted into a FEM entity by a meshing process using 3D hexahedral element as shown in Figure 8. The boundary condition was imposed to mitigate the tensile test by fixing one end with the other end having axial tensile load being applied as shown in Figure 9. It also assigned the properties of the material like young's modulus value which was obtained from the experimental value.

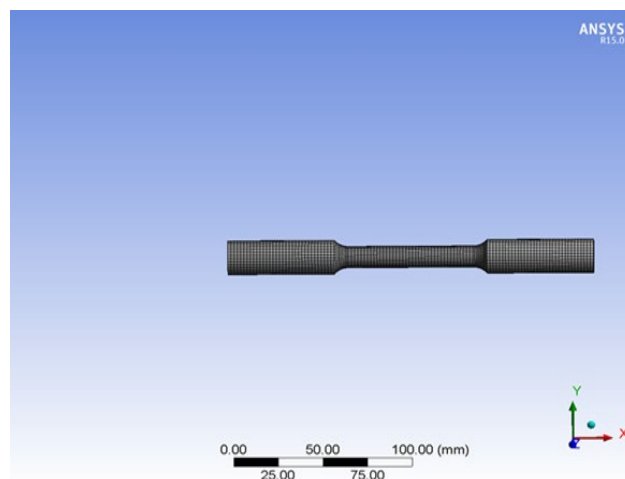


**Fig. 8:** FEA model of tensile test.

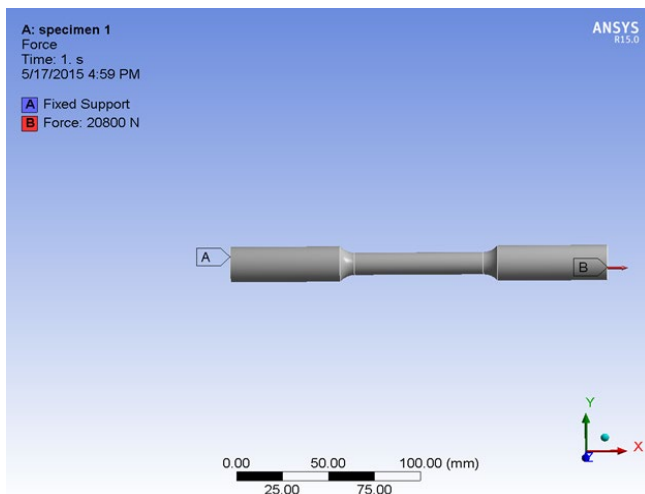


Fig. 9: Boundary conditions apply to model.

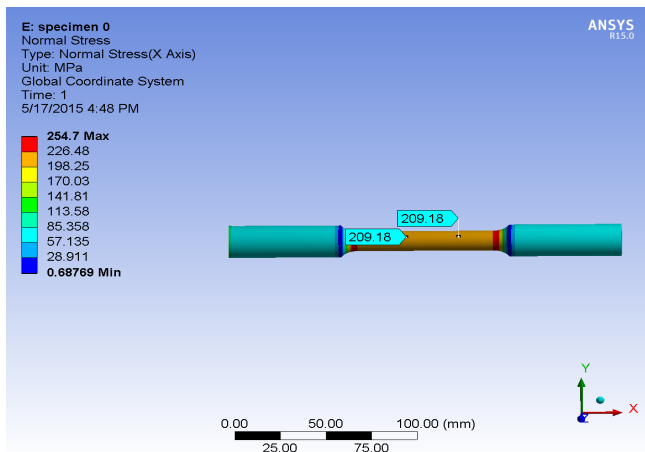


Fig. 10: Tensile test analysis of Al7075 alloy (unreinforced).

The tensile test analysis for specimen 1 with 2% B<sub>4</sub>C composite alloy was carried out. It was observed that tensile strength was obtained as 167.35 MPa at a near gauge length as shown in Figure 11.

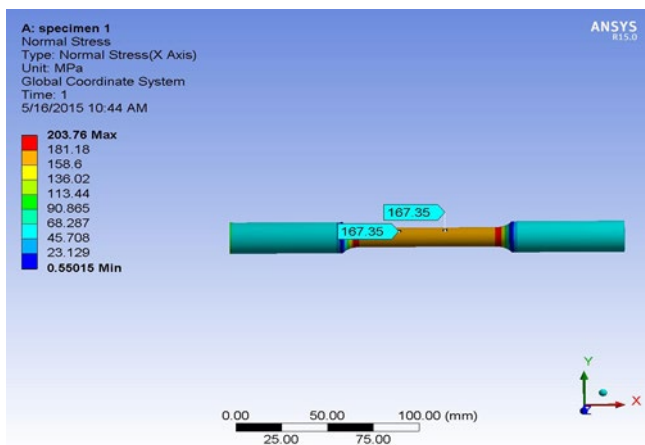


Fig. 11: Tensile test analysis of Al7075-2% Al<sub>2</sub>O<sub>3</sub>-2% B<sub>4</sub>C.

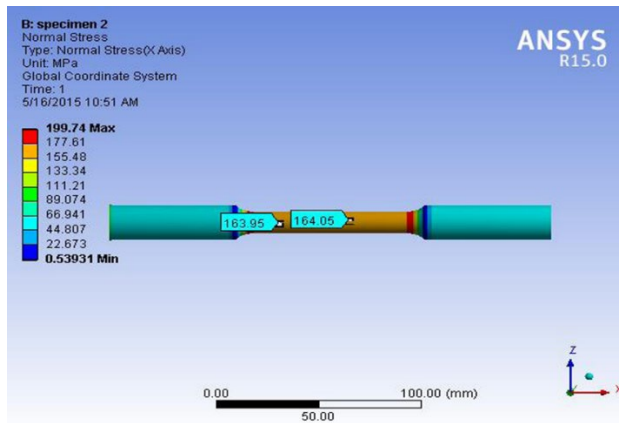


Fig. 12: Tensile test analysis of Al7075-2% Al<sub>2</sub>O<sub>3</sub>-4% B<sub>4</sub>C.

The tensile test analysis for specimen 2 with 4% B<sub>4</sub>C composite alloy was carried out. It was observed that tensile strength was obtained as 164 MPa at a near gauge length as shown in Figure 12. The tensile test analysis for specimen 3 with 6% B<sub>4</sub>C composite alloy was carried out. It was observed that tensile strength was obtained as 159.96 MPa at a near gauge length as shown in Figure 13.

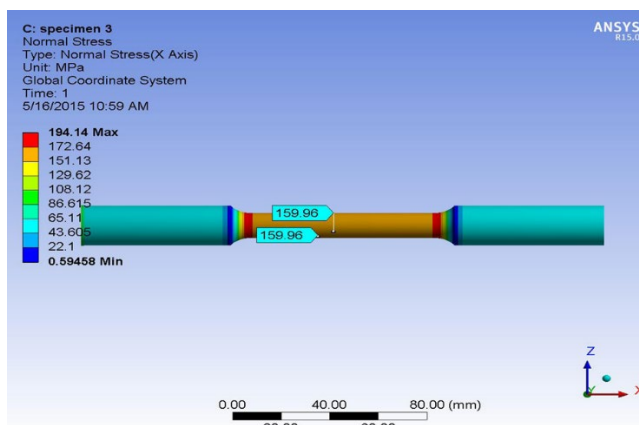


Fig. 13: Tensile test analysis of Al7075-2% Al<sub>2</sub>O<sub>3</sub>-6% B<sub>4</sub>C.

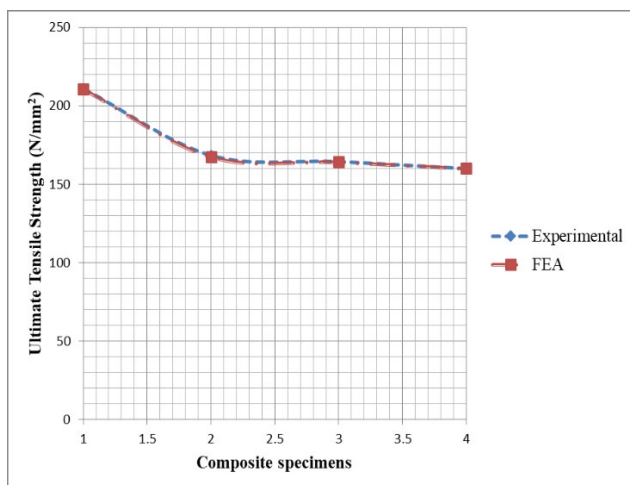


Fig. 14: Comparison between FEA and experimental results of tensile test.

The static structural tensile test was successfully

simulated in ANSYS. It was observed that both the FEA results and analytical results were correlated with each other as shown in Figure 14.

### 4.2 Compression

The static structural FEA wears analysis was carried out. A 3D CAD model was meshed using a 3D hexahedral element as shown in Figure 15. Boundary conditions were imposed as per the experimental simulation like the bottom end being fixed whereas the axial compression load 53400N was applied as shown in Figure 16.

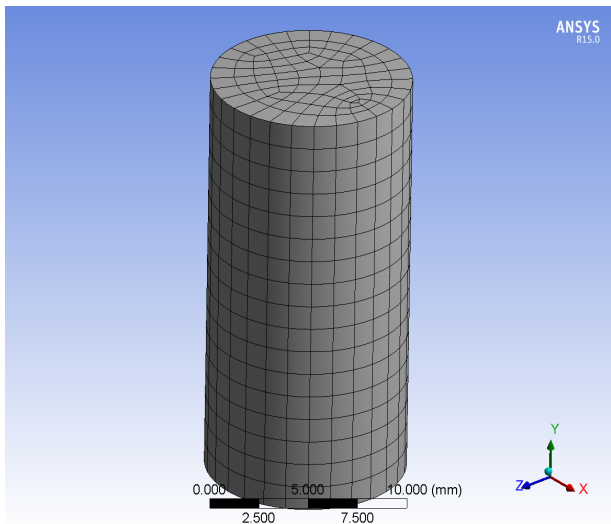


Fig. 15: FEA model of compression.

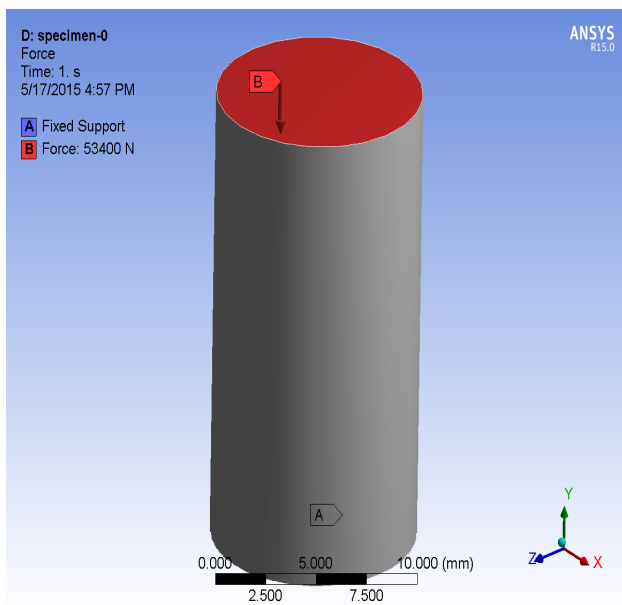


Fig. 16: Boundary conditions apply to model.

The compression test analysis for specimen Al7075 alloy was carried out. It was observed that nominal compression strength was obtained as -645.89 MPa as shown in Figure 17.

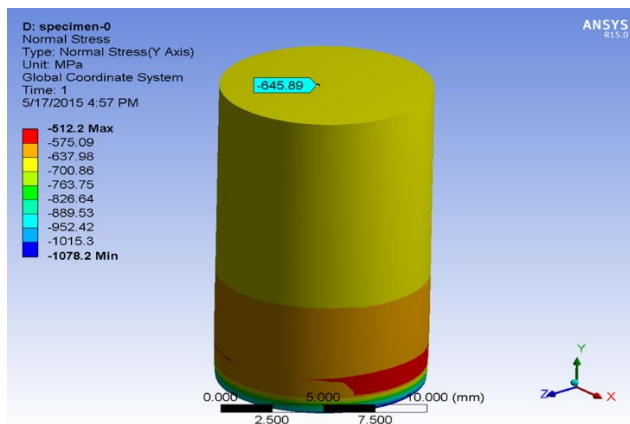


Fig. 17: Compression test analysis of Al 7075 alloy (Unreinforced).

The compression test analysis for specimen 2 with 2% B<sub>4</sub>C composite alloy was carried out. It was observed that nominal compression strength obtained was -689.43 MPa as shown in Figure 18.

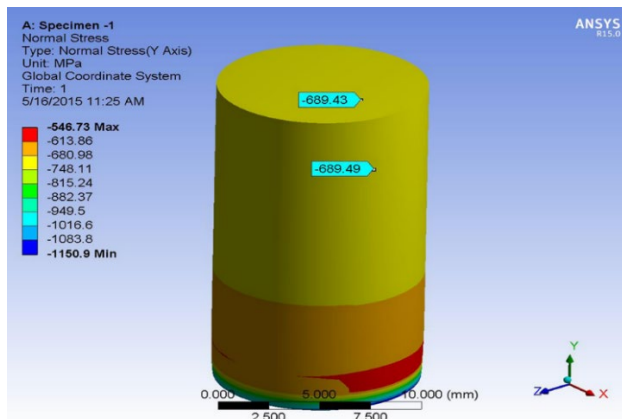


Fig. 18: Compression test analysis of Al7075-2% Al<sub>2</sub>O<sub>3</sub>-2% B<sub>4</sub>C.

The compression test analysis for specimen 3 with 4% B<sub>4</sub>C composite alloy was carried out. It was observed that nominal compression strength obtained was -889.7 MPa as shown in Figure 19.

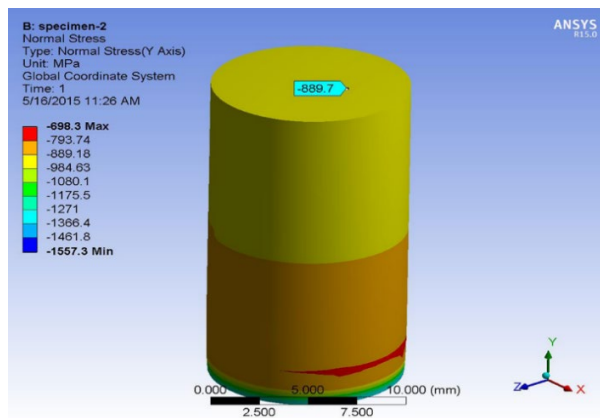
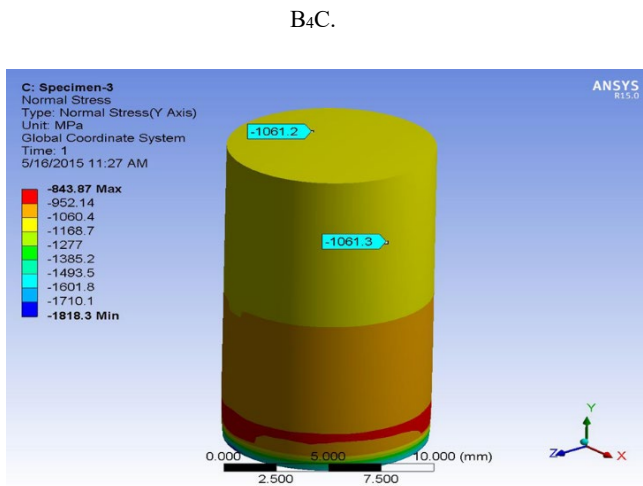


Fig. 19: Compression test analysis of Al7075-2% Al<sub>2</sub>O<sub>3</sub>-4%





**Fig. 20:** Compression test analysis of Al7075-2% Al<sub>2</sub>O<sub>3</sub>-6% B<sub>4</sub>C.

The compression test analysis for specimen 1 with 6% B<sub>4</sub>C composite alloy was carried out. It was observed that nominal compression strength obtained was -1061.2 MPa as shown in Figure 20. The static structural compression test was successfully simulated in ANSYS. It was observed that both FEA results and analytical results were correlated with as shown in Figure 21.

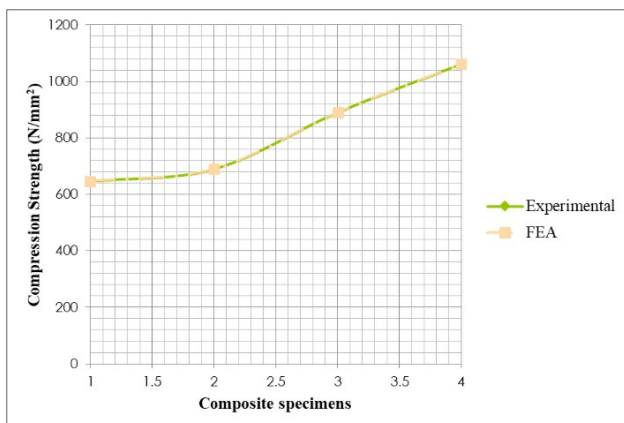


**Fig. 21:** Comparison between FEA and experimental results of compression test.

## 5. Conclusion

Research work has been carried out on **“Investigating the Mechanical Properties of Al 7075 Alloy for Automotive Applications: Synthesis and Analysis”**. Hybrid composites of multiple compositions was successfully formed using the stir casting technique. Standard specimens have been machined and these specimen components were subjected to various tests for characterization.

- The formed hybrid composites (Al/Al<sub>2</sub>O<sub>3</sub>/B<sub>4</sub>C) were examined under an optical microscope with different magnification factors to recognize the dispersion of Al<sub>2</sub>O<sub>3</sub> and B<sub>4</sub>C particles in the matrix, grain boundary and grain size, precipitate

formation on the grains.

- SEM micrographs showed that the fabricated Al7075 alloy composites contained B<sub>4</sub>C and alumina particles. XRD patterns were also used to distinguish between various elements and phases in B<sub>4</sub>C and alumina particles. These reinforcements improved the hardness and tensile properties while decreasing the ductility of the underlying Al7075 alloy matrix.
- When compared to an as-cast specimen, the created composites tensile strength, hardness, and yield strength have all increased as the weight percentage of Al<sub>2</sub>O<sub>3</sub> and B<sub>4</sub>C particles has grown.
- Al7075 alloy hybrid composites were successfully produced by the stir casting route to study its mechanical properties.
- The hardness resistance of the composites increased by increasing the amount of boron carbide in the matrix phase.
- Increasing the amount of boron carbide in the composite increased its compression strength and decreased its tensile strength.
- When compared to the matrix material, the produced composites' percentage increases in tensile strength, hardness, and yield strength were measured at 36.70%, 31.42%, and 33.99%, respectively.
- The FEA results revealed that they were correlated with the experimental values.
- Mechanical properties could be evaluated by varying the wt. % of the Al<sub>2</sub>O<sub>3</sub> reinforcement.

## References

- 1) Xavier, L.F., and Suresh, P. “Wear behavior of aluminum metal matrix composite prepared from industrial waste”, *The Scientific World Journal*, 2, pp 1–9. (2016) Doi:10.1155/2016/6538345.
- 2) Kumaraswamy, J., Vijaya Kumar and Purushotham, G. “A review on mechanical and wear properties of ASTM a 494 M grade nickel-based alloy metal matrix composites”, *Materials Today: Proceedings*, 37, pp 2027–2032. (2021) Doi: 10.1016/j.matpr.2020.07.499.
- 3) Karthikkumar, C., Baranirajan, R., Premnauth, I., and Manimaran, P. “Investigations on Mechanical properties of AL 8011 reinforced with micro B<sub>4</sub>C / Red Mud by Stir Casting Method”, *International Journal of Engineering Research and General Science*, 4 (2), PP-405-412. (2016).
- 4) Shaik Mujeeb Quader, Suryanarayana Murthy, B., and Pinninti Ravinder Reddy. “Processing and Mechanical Properties of Al<sub>2</sub>O<sub>3</sub> and Red Mud Particle Reinforced AA6061 Hybrid Composites”, *Journal of Minerals and Materials Characterization and Engineering*, 4, pp 135-142 (2016).

- 5) Jayappa, K., Kumar, V. and Purushotham, G. "Effect of reinforcements on mechanical properties of nickel alloy hybrid metal matrix composites processed by sand mold technique", *Applied Science and Engineering Progress*, 14(1), pp. 44–51. (2021). DOI: 10.14416/j.asep.2020.11.001.
- 6) Campbell. "Manufacturing technology for aerospace structural materials", Butterworth-Heinemann publications, ISBN: 978-1-85-617495-4, Elsevier Inc. (2006).
- 7) Rana, R. S., Rajesh Purohit, and Das, S. "Review of recent Studies in Al matrix composites", *International Journal of Scientific & Engineering Research*, 3(6). (2012).
- 8) Bhaskar, H.B, and Abdul sharief. "Tribological Properties of Aluminium 2024 Alloy–Beryl Particulate MMC's", *Bonfring International Journal of Industrial Engineering and Management Science*, 2 (4), pp 143-147. (2012)
- 9) Reddappa, H. N., Suresh, K. R., Niranjana, H. B, and Satyanarayana, K. G. "Effect of Aging on Mechanical and Wear Properties of Beryl Particulate Reinforced Metal Matrix Composites", *Journal of Engineering Science and Technology*, 9(4), pp 455-462. (2014).
- 10) Jayappa, K., Kumar, V. and Purushotham, G. "Thermal analysis of nickel alloy/Al<sub>2</sub>O<sub>3</sub>/TiO<sub>2</sub> hybrid metal matrix composite in automotive engine exhaust valve using FEA method", *Journal of Thermal Engineering*, 7(3), pp. 415-428. (2021). Doi: 10.18186/thermal.882965.
- 11) Radhika, N., Subramanian, R, and Venkat Prasat, S. "Tribological Behaviour of Aluminium/Alumina/Graphite Hybrid Metal Matrix Composite Using Taguchi's Techniques", *Journal of Minerals & Materials Characterization & Engineering*, 10(5), pp. 427-443. (2011).
- 12) Sujana, D., Oo, Z., Rahman, M.E., Maleque, M.A, and Tan, C.K. "Physio-mechanical Properties of Aluminium Metal Matrix Composites Reinforced with Al<sub>2</sub>O<sub>3</sub> and SiC", *International Journal of Engineering and Applied Sciences*, 6, pp- 288-291. (2012).
- 13) Davis, J.R. *Aluminum and Aluminum Alloys*, ASM International, pp 351-416, Doi:10.1361/autb2001 p351.
- 14) Kumaraswamy, J., Vijaya Kumar and Purushotham, G. "Evaluation of the microstructure and thermal properties of (ASTM A 494 M grade) nickel alloy hybrid metal matrix composites processed by sand mold casting", *International Journal of Ambient Energy*, 42, pp. 1-10. (2021). DOI:10.1080/01430750.2021.1927836.
- 15) Rahimi, M., Fojan, P., Gurevich, L, and Afshari, A. "Aluminium alloy 8011: Surface characteristics", *Applied Mechanics and Materials*, 719-720, pp 29-37.
- 16) Valmir Martins Monteiro, Saulo Brinco Diniz, Bruna Godoi Meirelles, Luis Celso da Silva, Andersan dos Santos Paula. "Microstructural and Mechanical Study of Aluminium Alloys Submitted To Distinct Soaking Times During Solution Heat Treatment", *Tecnol. Metal. Mater. Miner.*, São Paulo, 11(4), pp 332-339. (2014). Doi: /10.4322/tmm.2014.047.
- 17) Marek, J., Karlík, M., Sláma, P. "Textures of Aluminum Alloy Thin Sheets for Heat Exchanger Fins", *Materials Structure*, 8 (1), Pp 25-28. (2001)
- 18) Bauxite residue management: best practice, international aluminum Institute (IAI). (2015). www. World-aluminum.org.
- 19) Sreenivasrao, K. V., Anil, K. C., Girish, K. G. and Akash. "Mechanical characterization of red mud reinforced Al-8011 matrix composite", *ARPN Journal of Engineering and Applied Sciences*, 11(1), pp-229-234. (2016)
- 20) Anil, K.C., Kumaraswamy, J., Akash, and Sanman, S. "Experimental arrangement for estimation of metal-mold boundary heat flux during gravity chill casting", *Materials Today: Proceedings*, (2022) Doi: 10.1016/j.matpr.2022.07.399.
- 21) H. Sosiati, N.D.M. Yuniar, D. Saputra, and S. Hamdan, "The Influence of Carbon Fiber Content on the Tensile, Flexural, and Thermal Properties of the Sisal/PMMA Composites" *EVERGREEN Joint Journal of Novel Carbon Resource Sciences & Green Asia Strategy*, Vol. 9(1) pp32-40 (2022). doi.org/10.5109/4774214.
- 22) Anthony Chukwunonso Opia, Mohd Kameil Abdul Hamid, Samion Syahrullail, Audu Ibrahim Ali, Charles N. Johnson, Ibham Veza, Mazali Izhari Izmi, Che Daud Zul Hilmi, Abu Bakar Abd Rahim, "Tribological Behavior of Organic Anti-Wear and Friction Reducing Additive of ZDDP under Sliding Condition: Synergism and Antagonism Effect" *EVERGREEN Joint Journal of Novel Carbon Resource Sciences & Green Asia Strategy*, Vol. 9(2) pp246-253 (2022). doi.org/10.5109/4793628.
- 23) Muhammad Miqdad, Anne Zulfia Syahrail, "Effect of Nano Al<sub>2</sub>O<sub>3</sub> Addition and T6 Heat Treatment on Characteristics of AA 7075 / Al<sub>2</sub>O<sub>3</sub> Composite Fabricated by Squeeze Casting Method for Ballistic Application" *EVERGREEN Joint Journal of Novel Carbon Resource Sciences & Green Asia Strategy*, Vol. 9(2) pp531-537 (2022). doi.org/10.5109/4794184.
- 24) Mr. Dilip Choudhari, Dr. Vyasraj Kakhhandki, "Characterization and Analysis of Mechanical Properties of Short Carbon Fiber Reinforced Polyamide66 Composites" *EVERGREEN Joint Journal of Novel Carbon Resource Sciences & Green Asia Strategy*, Vol. 08, Issue 04, pp768-776, (2021). doi.org/10.5109/4742120.
- 25) Anthony Chukwunonso Opia, Mohd Kamei Abdul Hamid, Samion, Syahrullail, Charles A. N. Johnson, Abu Bakar Rahim, Mohammed B. Abdulrahman, "Nano-Particles Additives as a Promising Trend in Tribology: A Review on their Fundamentals and

- Mechanisms on Friction and Wear Reduction” EVERGREEN Joint Journal of Novel Carbon Resource Sciences & Green Asia Strategy, Vol. 8(4) pp777-798 (2021). doi.org/10.5109/4742121.
- 26) Anil K C, Kumaraswamy J, Mahadeva Reddy, Mamatha K M, “Air Jet Erosion studies on Aluminum - Red Mud Composites using Taguchi Design” EVERGREEN Joint Journal of Novel Carbon Resource Sciences & Green Asia Strategy, Vol. 10(1) pp130-138 (2023). doi.org/10.5109/6781059
- 27) Sharan kumar, Akash, Anil K C, Kumaraswamy J, “Solid Particle Erosion Performance of Multi-layered Carbide Coatings (WC-SiC-Cr<sub>3</sub>C<sub>2</sub>)” EVERGREEN Joint Journal of Novel Carbon Resource Sciences & Green Asia Strategy, Vol. 10(2) pp813-819 (2023). doi.org/10.5109/6792833.
- 28) Harish R S, Sreenivasa Reddy M, Kumaraswamy J, Wear characterization of Al7075 Alloy hybrid composites, Journal of Metallurgical and Materials Engineering, Vol. 28 (2), pp. 291-303. https://doi.org/10.30544/821.
- 29) J. Kumaraswamy et al., "Thermal Analysis of Ni-Cu Alloy Nanocomposites Processed by Sand Mold Casting," Advances in Materials Science and Engineering, vol. 2022, Article ID 2530707, 11 pages, 2022. https://doi.org/10.1155/2022/2530707
- 30) R.S. Harish, M. Sreenivasa Reddy and J. Kumaraswamy, Mechanical behaviour of Al7075 alloy Al<sub>2</sub>O<sub>3</sub>/E-Glass hybrid composites for automobile applications, Materials Today: Proceedings, Volume 72, Part 4, 2023, Pages 2186-2192. https://doi.org/10.1016/j.matpr.2022.08.460
- 31) J. Kumaraswamy, K.C. Anil and V. Shetty, Development of Ni-Cu based alloy hybrid composites through induction furnace casting, Materials Today: Proceedings, Vol. 72, pp. 2268-2274. https://doi.org/10.1016/j.matpr.2022.09.215